

Transport of the repulsive Bose-Einstein condensate in a double-well trap: interaction impact and relation to Josephson effect

V O Nesterenko¹, A N Novikov¹ and E Suraud²

¹Bogoliubov Laboratory of Theoretical Physics, Joint Institute for Nuclear Research, Dubna, Moscow region, 141980, Russia

E-mail: nester@theor.jinr.ru

²Laboratoire de Physique Quantique, Université Paul Sabatier, 118 Route de Narbonne, 31062 cedex, Toulouse, France

Abstract. Two aspects of the transport of the repulsive Bose-Einstein condensate (BEC) in a double-well trap are inspected: impact of the interatomic interaction and analogy to the Josephson effect. The analysis employs a numerical solution of 3D time-dependent Gross-Pitaevskii equation for a total order parameter covering all the trap. The population transfer is driven by a time-dependent shift of a barrier separating the left and right wells. Sharp and soft profiles of the barrier velocity are tested. Evolution of the relevant characteristics, involving phase differences and currents, is inspected. It is shown that the repulsive interaction substantially supports the transfer making it possible i) in a wide velocity interval and ii) three orders of magnitude faster than in the ideal BEC. The transport can be approximately treated as the d.c. Josephson effect. A dual origin of the critical barrier velocity (break of adiabatic following and d.c.-a.c. transition) is discussed. Following the calculations, robustness of the transport (d.c.) crucially depends on the interaction and barrier velocity profile. Only soft profiles which minimize undesirable dipole oscillations are acceptable.

PACS numbers: 03.75.Lm, 03.75.Kk

Keywords: trapped Bose-Einstein condensate, quantum transport, Josephson effect.

1. Introduction

The population transfer is a typical problem met in various branches of physics (ultracold gases and condensates [1, 2, 3, 4, 5, 6, 7, 8, 9], atomic and molecular physics [10], etc.). The problem is easily solvable, if it is linear and accepts an adiabatic evolution, see e.g. the Landau-Zener scenario [11, 12]. However, if there are significant nonlinear effects or/and we need a rapid but robust transfer, the problem becomes nontrivial, like e.g. in the irreversible nonlinear transport (NLT) of Bose-Einstein condensate (BEC) in multi-well traps [13, 14]. The trapped BEC is especially suited for investigation of nonlinear transport because BECs features, including the interaction-induced nonlinearity, can be precisely controlled and manipulated. Besides, by driving the trap parameters one can simulate various transport protocols.

Despite numerous experimental and theoretical studies (see early [1, 2, 3, 4, 5, 6] and recent [7, 15] reviews), some important NLT features yet poorly understood. In particular, it is not well established in which cases the nonlinearity favors the transport and how essential is the effect.

In the present study, we address these general questions for a typical NLT scheme: an external Bose Josephson junction (EBJJ) produced in a double-well trap. Here the left and right BEC fractions are coupled through the barrier separating the tap. The nonlinear effects are caused by interaction between BEC atoms. The NLT is a population inversion driven by converting the trap from initial to final (opposite) asymmetric configurations. Nowadays such INTL is a routine experimental operation which can be produced by various methods: from familiar Rabi oscillations (π pulses) [16] and (quasi)adiabatic population transfer [11, 12, 14] to modern shortcut-to-adiabaticity methods (see review [7] and particular relevant options [17, 18, 19]) promising a fast and robust population inversion. The goal of the present study is to use this simple operation for exploration of: i) strong nonlinear effects predicted for this configuration within a simple two-mode model [14], ii) analogy between NLT and d.c. (direct current) Josephson effect in superconductors [20], predicted [21, 22, 23, 24, 25, 26] and observed [27] in EBJJ.

For this purpose, the three-dimensional (3D) time-dependent Gross-Pitaevskii equation (GPE) [28] for the total order parameter covering both left and right parts of the condensate in a double-well trap is numerically solved. The calculations are free from the two-mode approximation (TMA) [29] and other simplifications used in our previous estimations [14]. Furthermore, our study closely follows conditions and parameters of Heidelberg's experiments [31, 32], thus providing atypical but realistic picture. The population transfer is determined by a time-dependent barrier shift driving the system between initial and final asymmetric configurations. This technique allows to reach simultaneously two aims: i) exercise a generalized Landau-Zener/Rosen-Zener transport protocol implemented in our previous study [14] and ii) simulate an external current required for generation of Josephson d.c. in EBJJ [24]. To highlight nonlinear effects, the dynamics of ideal and repulsive BEC is compared.

In our previous TMA study, a strong support of the transport by the repulsive interaction was found [14]. It was shown that the interaction leads to a wide range (plateau) of the process rates, where a complete (quasi)adiabatic transport is realized. In the present study, we test these results within a more realistic model beyond the TMA. The scale of the nonlinear effects is estimated for the particular Heidelberg setup [31, 32]. It is shown that the repulsive BEC can be transferred by 3 orders of magnitude faster than the ideal condensate. A pollution of NLT by dipole oscillations is estimated and a smooth velocity regime moderating this problem is proposed.

In the second part of our exploration, the NLT is compared with the Josephson d.c. and a.c. effects [20] represented for BEC by equations [24]

$$I = I_0 \sin(\theta), \quad \dot{\theta} = \frac{\Delta\mu}{h}, \quad (1)$$

where I is the supercurrent, I_0 is its critical value and $\Delta\mu$ is the difference between chemical potentials of the wells. As predicted [24] and then experimentally observed [27], the d.c. can be generated in EBJJ by an adiabatic movement of the barrier across the trap with a constant velocity, thus simulating the driving current. The shift can drive the trap from asymmetric to symmetric configuration [27] or vice versa [20]. The adiabatic evolution assumes that the system change is so slow that tunneling of atoms between the wells is sufficient to lock $\Delta\mu$ to zero. When the shift is over, we get the Josephson d.c. I driven by the phase difference θ . The critical current I_0 should be proportional to the critical velocity v^{crit} of the barrier shift. Above this velocity, the adiabatic flow breaks down, the nonzero $\Delta\mu$ develops, and the process becomes of a.c. character with $I = I_0 \sin(\Delta\mu t/\hbar)$ [24, 25, 26].

It is easy to see that this scenario corresponds to an adiabatic NLT described within the TMA in our previous study [14]. The plateau in the transport rates [14] is just the region $I < I_0$ where the adiabatic evolution takes place. The critical rate [14] marking the break of the adiabatic transport seems to correspond to v^{crit} and I_0 in [24, 27]. The analogy should take place despite the population transfer in [14] is driven not by the barrier shift but by another technique generalizing Landau-Zener and Rosen-Zener schemes. Both scenarios have to be physically similar since they satisfy the principle requirements: weak coupling, inherent phase difference, and adiabatic evolution.

In the present study, we continue analysis of d.c. and a.c. in EBJJ but now with the accent to nonlinear effects. As compared to the previous studies [22, 23, 24, 25, 26] which were limited to inspection of the population imbalance z and chemical potential difference $\Delta\mu$, we also scrutinize the evolution of the phase difference θ , a principle factor of the Josephson dynamics. In particular, we provide a detailed analysis of θ near v^{crit} . Also, a pollution effect of the dipole oscillations is estimated. It is shown that the constant barrier velocity [24] results in strong oscillations which greatly smear the process and complicate the analysis. Thus, a soft velocity profile is proposed to circumvent this trouble. It is shown that the repulsive interaction and soft velocity profile make the NLT (and d.c./a.c.) much more suitable for the analysis and experimental observation.

Note that last years EBJJ is widely used in diverse actual areas (shortcuts to adiabaticity and optimal control [7, 15], spin squeezing, entanglement and quantum metrology [33, 34], Josephson dynamics in spin-orbit BEC [35], etc). At the same time, investigations of d.c./a.c. regimes in EBJJ are yet sparse [36], despite interesting flaring similarity of d.c. with adiabatic population transfer scenarios. The present detailed study of a.c./d.c. in a double-well trap aims to supply partly this gap.

The paper is organized as follows. The theory and calculation framework are outlined in Sec. 2. The results are discussed in Sec. 3. The summary is given in Sec. 4.

2. Calculation scheme

2.1. Trap setup and well populations

The calculations are performed within the 3D time-dependent Gross-Pitaevskii equation (GPE) [28]

$$i\hbar \frac{\partial \Psi}{\partial t}(\mathbf{r}, t) = \left[-\frac{\hbar^2}{2m} \nabla^2 + V(\mathbf{r}, t) + g_0 |\Psi(\mathbf{r}, t)|^2 \right] \Psi(\mathbf{r}, t) \quad (2)$$

for the total order parameter $\Psi(\mathbf{r}, t)$ describing BEC in both left and right wells of the trap. Here $g_0 = 4\pi\hbar^2 a_s/m$ is the interaction parameter, a_s is the scattering length, and m is the atomic mass. The trap potential

$$\begin{aligned} V(\mathbf{r}, t) &= V_{\text{con}}(\mathbf{r}) + V_{\text{bar}}(x, t) \\ &= \frac{m}{2}(\omega_x^2 x^2 + \omega_y^2 y^2 + \omega_z^2 z^2) \\ &\quad + V_0 \cos^2(\pi(x - x_0(t))/q_0) \end{aligned} \quad (3)$$

includes the anisotropic harmonic confinement and the barrier in x -direction, whose position is driven by the control function $x_0(t)$ [24, 26]; V_0 is the barrier height and q_0 determines the barrier width.

Following conditions of the Heidelberg experiment [31, 32] (where Josephson oscillations (JO) and macroscopic quantum self-trapping (MQST) have been observed), we consider BEC of $N=1000$ ^{87}Rb atoms with $a_s = 5.75$ nm. The trap frequencies are $\omega_x = 2\pi \times 78$ Hz, $\omega_y = 2\pi \times 66$ Hz, $\omega_z = 2\pi \times 90$ Hz, i.e. $\omega_y + \omega_z = 2\omega_x$. The barrier parameters are $V_0 = 420 \times h$ Hz and $q_0 = 5.2$ μm . For the symmetric trap ($x_0(t)=0$), the distance between the centers of the left and right wells is $d=4.4$ μm . This setup has been earlier used in our exploration of JO/MQST in a weak and strong coupling [39]. It corresponds to so called Josephson (classical) regime when quantum fluctuations of both population imbalance and phase difference are not essential.

The static solutions of GPE are found within the damped gradient method [37] while the time evolution is computed within the time-splitting technique [38]. The total order parameter $\Psi(\mathbf{r}, t)$ is determined in a 3D cartesian grid. The conservation of the number of atoms, $\int_{-\infty}^{\infty} d\mathbf{r}^3 |\Psi(\mathbf{r}, t)|^2 = N$, is directly fulfilled by using an explicit unitary

propagator. No time-space factorization of the order parameter is implemented. The conservation of the total energy E is controlled.

The populations of the left (L) and right (R) wells are computed as

$$N_j(t) = \int_{-\infty}^{+\infty} dr^3 |\Psi_j(\mathbf{r}, t)|^2, \quad (4)$$

with $j = L, R$, $\Psi_L(\mathbf{r}, t) = \Psi(x \leq x_0(t), y, z, t)$, $\Psi_R(\mathbf{r}, t) = \Psi(x \geq x_0(t), y, z, t)$ and $N_L(t) + N_R(t) = N$. The normalized population imbalance is

$$z(t) = (N_L(t) - N_R(t))/N. \quad (5)$$

The NLT to be considered means that initial ($t=0$) BEC populations $N_L(0) > N_R(0)$ are inverted during the time T to the final populations $N_L(T) < N_R(T)$ where $N_L(T) = N_R(0)$ and $N_R(T) = N_L(0)$. The initial stationary *asymmetric* BEC state is produced by adjusting the barrier right-shift ($x(0) > 0$) so as to provide the required initial populations $N_L(0)$ and $N_R(0)$. The NLT is achieved by a barrier left shift from $x(0)$ to $x(T) = -x(0)$ with the shift velocity $v(t)$. Thus the trap asymmetry is changed to the opposite one.

Two velocity time profiles are used: i) the sharp rectangular one with the constant $v_c(t) = v_0^c$ at $0 < t < T$ and $v_c(t) = 0$ beyond the transfer time, and ii) the soft one $v_s(t) = v_0^s \cos^2(\frac{\pi}{2} + \frac{\pi t}{T})$ with $v_s(0) = v_s(T) \sim 0$ and $v_s(T/2) = v_0^s$. For the total barrier shift $D = 2x(0)$ in the inversion process of duration T , the velocity amplitudes are $v_0^c = D/T$ and $v_0^s = 2D/T$. The average velocities $v_a = D/T$ are:

$$v_a^c = v_0^c, \quad v_a^s = v_0^s/2. \quad (6)$$

The constant profile $v_c(t)$ was used in previous studies [24, 26]. It sharply changes from 0 to v_0^c at $t=0$ and back at $t=T$ and, in this sense, is not adiabatic. As shown below, the sharp changes cause undesirable dipole oscillations which can significantly pollute the population transfer. The second profile $v_s(t)$ is softer and thus closer to the adiabatic evolution.

The NLT quality is characterized by its completeness $P = -z(T)/z(0)$ (the ratio of the final and initial population imbalance) and noise $n = A_d/N$ where A_d is amplitude of dipole oscillations in the final state, i.e. $A_d = \max\{N_{L,R}\} - \min\{N_{L,R}\}$ for $t > T$.

Note that previous studies used 3D [24] and 1D [26] numerical time-dependent GPE simulations as well.

2.2. Phases

The phases $\phi_j(t)$ of the left and right BEC fractions are defined as [39]

$$\varphi_j(t) = \arctan \frac{\gamma_j(t)}{\zeta_j(t)} \quad (7)$$

with the averages

$$\varsigma_j(t) = \frac{1}{N_j} \int_{-\infty}^{+\infty} dr^3 \text{Im}(\Psi_j(\mathbf{r}, t)) |\Psi_j(\mathbf{r}, t)|^2, \quad (8)$$

$$\chi_j(t) = \frac{1}{N_j} \int_{-\infty}^{+\infty} dr^3 \text{Re}(\Psi_j(\mathbf{r}, t)) |\Psi_j(\mathbf{r}, t)|^2. \quad (9)$$

Since computation of the phase time evolution through arctan may be cumbersome, we use (11) only for the static case while the time evolution is calculated through the phase increments $\varphi_j(t + \delta t) \approx \varphi_j(t) + \delta\varphi_j(t)$ for a small time step δt . Namely, we use

$$\delta\varphi_j(t) = \sqrt{\frac{[\delta\varsigma_j(t)]^2 + [\delta\chi_j(t)]^2}{\varsigma_j^2(t + \delta t) + \chi_j^2(t + \delta t)}} \quad (10)$$

with $\delta\varsigma_j(t) = \varsigma_j(t + \delta t) - \varsigma_j(t)$, $\delta\chi_j(t) = \chi_j(t + \delta t) - \chi_j(t)$. The phase difference is

$$\theta(t) = \varphi_R(t) - \varphi_L(t). \quad (11)$$

2.3. Energy estimations

To discriminate weak and strong couplings between BEC fractions, it is instructive to compare the energy of the occupied state with the barrier height V_0 . Since the barrier takes place in x-direction, only the part of the ground state energy in the same direction is relevant. In the linear case ($g_0=0$), the total ground state energy reads as in anisotropic harmonic oscillator, $\mu_0 = \mu_{x0} + \mu_{yo} + \mu_{z0}$, and its relevant x-part is

$$\mu_{x0} = \mu_0 - \frac{\hbar}{2}(\omega_y + \omega_z) = \mu_0 - \hbar\omega_x = \alpha\mu_0 \quad (12)$$

where the relation $\omega_y + \omega_z = 2\omega_x$ [31, 32] is used. The numerical GPE estimation gives $\alpha = \mu_{x0}/\mu_0 \approx 3/4$ [39].

In the nonlinear case ($g_0 \neq 0$), the estimation of μ_x is straightforward for 1D system but demanding for 3D case considered here. So we use the simple ansatz

$$\mu_x = \alpha\mu \quad (13)$$

where μ is the total *nonlinear* ground state energy and $\alpha \approx 3/4$ as in the linear case. This phenomenological relation was shown to be accurate in investigation of the evolution of JO/MQST dynamics under the transition from a weak to a strong coupling [39]. In this study, it is used only for illustrative aims, namely for the comparison with the barrier height V_0 in Fig. 1.

The energies μ_0 and μ can be treated as chemical potentials in the Josephson setup [1, 2, 3, 4]. In the rapid evolution of the system, initiated by the barrier shift, the difference between chemical potentials of the left and right wells, $\Delta\mu = \mu_L - \mu_R$, can be created [24]. In NLT, $\Delta\mu$ can be estimated through $\dot{\theta}$, see Eq. (1).

2.4. Josephson current

The Josephson current is defined as

$$I(t) = -\frac{\dot{z}(t)}{2} = -\frac{\dot{N}_L(t)}{N} = \frac{\dot{N}_R(t)}{N}. \quad (14)$$

This explicit current may be compared to an approximate one

$$\tilde{I}(t) = I_0 \sqrt{1 - z(t)^2} \sin \theta(t) \quad (15)$$

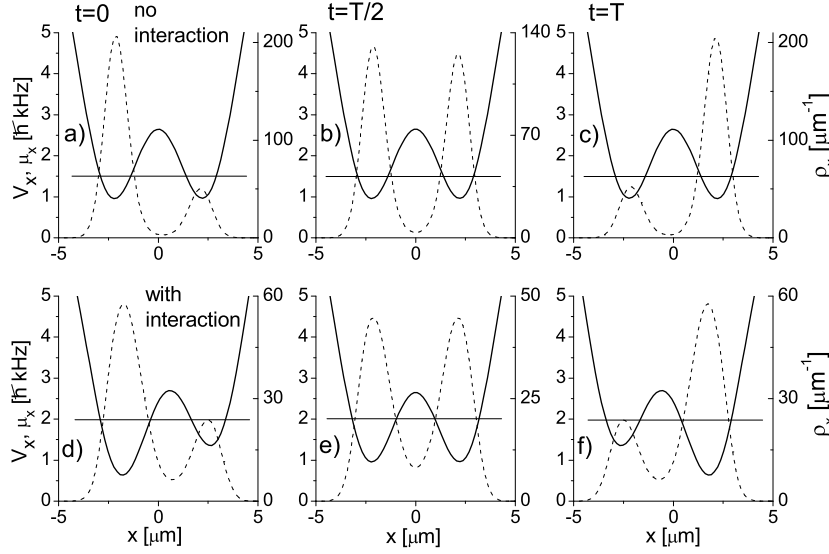


Figure 1. The double-well trap potential $V_x(x)$ (bold curve), BEC density $\rho_x(x)$ (dash curve), estimated ground state energy μ_x (solid strait line) at the initial ($t=0$), intermediate ($t=T/2$) and final inverse ($t=T$) states of the adiabatic inversion, calculated without (upper plots) and with (bottom plots) the repulsive interaction between BEC atoms. In both cases, the initial populations of the left and right wells are $N_L(0)=800$ and $N_R(0)=200$.

following from the first of the GPE-TMA equations [14, 21, 23, 29]:

$$\dot{z} = -2K\sqrt{1-z^2}\sin\theta, \quad (16)$$

$$\dot{\theta} = \frac{\Delta\mu}{2} + K\frac{z}{\sqrt{1-z^2}}\cos\theta + \frac{NU}{2}z. \quad (17)$$

Here I_0 is the EBJJ critical current, K is the coupling between BEC fractions through the barrier, U is the interaction between BEC atoms inside the trap wells. In the TMA, we have $I_0 = 2K$. Eqs. (16)-(17) are mathematically similar to those for resonantly generated coherent modes [30]. What is important for our aims, Eqs. (16)-(17) remind the Josephson equations (1).

In our study, we get the population imbalance $z(t)$, phase difference $\theta(t)$ and currents $I(t)$ and \tilde{I}/I_0 not from (16)-(17) but from a direct solution of the GPE (2). Then the comparison of the explicit (14) and approximate (15) currents at the reasonable point, say at $t = T/2$, allows to estimate the critical current I_0 .

3. Results and discussion

3.1. Confinement, density and chemical potential

Figure 1 exhibits the trap potential in x-direction,

$$V_x(x, t) = \frac{m}{2}\omega_x^2 x^2 + V_0 \cos^2(\pi(x - x_0(t))/q_0), \quad (18)$$

calculated for the initial $t=0$, intermediate $t=T/2$ and final $t=T$ times of the inversion process. For the same times, the BEC density profile in x-direction,

$$\rho(x, t) = \int_{-\infty}^{+\infty} dy dz |\Psi(x, y, z, t)|^2, \quad (19)$$

obtained for an adiabatic inversion of a long duration T is shown. The ideal and repulsive BECs with $N=1000$ atoms are considered. Following the plots a) and d), the initial populations of the left and right wells are $N_L(0)=800$ and $N_R(0)=200$ with the population imbalance $z(0)=0.6$. An adiabatic evolution provides a robust population inversion to final state with $N_L(T)=200$, $N_R(T)=800$ and $z(T)=-0.6$. At the intermediate time $t=T/2$, the trap and populations are symmetric. The initial state is stationary by construction. The intermediate and final states, being obtained adiabatically, can be also treated as stationary.

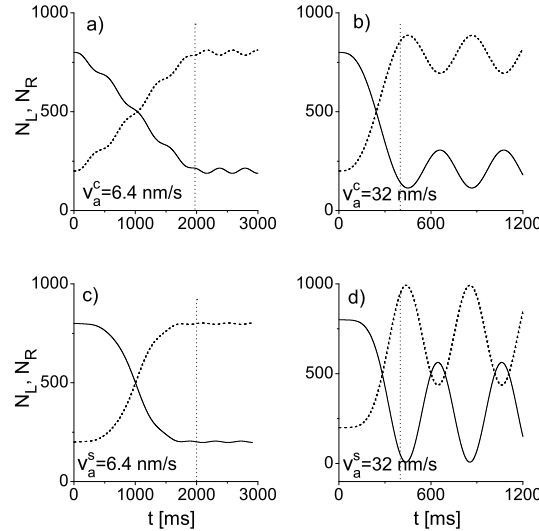


Figure 2. Evolution of populations $N_L(t)$ (solid curve) and $N_R(t)$ (dash curve) in the *ideal* (no interaction) BEC, calculated at the initial $N_L(0)=800$, $N_R(0)=200$ and $z(0)=0.6$. Durations of the barrier shifts $T=2$ s (a,c) and 0.40 s (b,d) are marked by vertical dotted lines. The transfers with the constant $v^c(t)$ (a,b) and soft $v_s(t)$ (c,d) velocity profiles are considered (with the same average velocities as indicated).

Upper plots of Fig. 1 show that for getting the initial $z(0)=0.6$ in the ideal BEC, a small trap asymmetry with $x_0(0)=0.0064 \mu\text{m}$ is sufficient. The overlap of the left and right parts of the condensate at the center of the trap is very small. The chemical potential μ_x from (12) lies much below the barrier top. The energy difference between the ground and first excited states at the mid of the transfer (plot b)) is $\Delta\mu(T/2)/h = 5$ Hz, i.e. much smaller than the well depths and trap frequencies. Altogether all these factors indicate a weak coupling case.

For the repulsive BEC (bottom plots), the initial $N_L(0)=800$ and $N_R(0)=200$ are obtained at a much larger asymmetry with $x_0(0)=0.5 \mu\text{m}$. The energy splitting $\Delta\mu(T/2)/h$ reaches 36 Hz. The repulsive interaction significantly increases the chemical

potential μ_x (13) and thus the coupling between the left and right BEC fractions. In this case, to get the initial *stationary* population imbalance $z(0)=0.6$, one should appreciably weaken the coupling by the corresponding increasing the asymmetry. As compared to the ideal BEC, the repulsive condensate has wider density bumps which significantly overlap at the center of the trap. The coupling between the left and right BEC fractions is not weak anymore, though the NLT considered below is yet realized through tunneling.

3.2. Linear and nonlinear dynamics

Some examples of the time evolution of the populations $N_{L,R}(t)$ in the ideal BEC are given in Fig. 2. The evolution is driven by the barrier shift with the rectangular $v_c(t)$ (upper plot) and soft $v_s(t)$ (bottom plots) velocity profiles. In both cases, the same average velocities are used. The total barrier shift is $D=12.8$ nm. It is seen that, at low (adiabatic) velocities corresponding to a long time $T=2$ s (plots a,c)), we get a robust population inversion. The final state is about stationary for $v_s(t)$ and somewhat spoiled by dipole oscillations for $v_c(t)$. The latter is caused by the sharp change of $v_c(t)$ at the beginning and end of the process. In this sense, the $v_s(t)$ -transfer is softer and more adiabatic. Following plots b,d), the inversion becomes worse or even breaks down at high velocities.

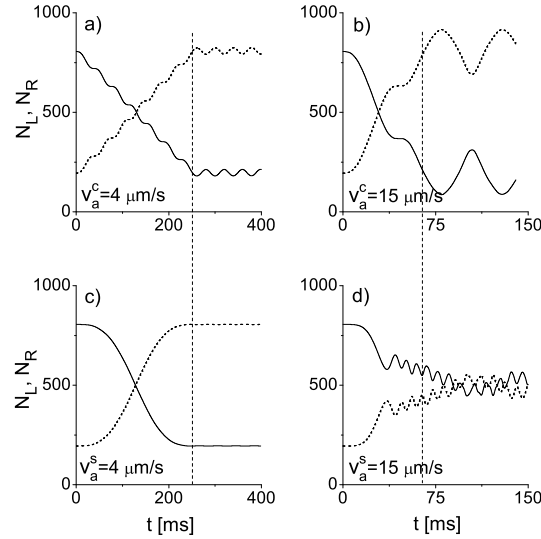


Figure 3. The same as in Fig. 2 but for the repulsive BEC. The barrier shift durations are $T=0.25$ s (a,c) and 0.067 s (b,d).

In Fig. 3, similar examples are given for the repulsive BEC. At first glance, the non-linear evolution resembles the linear one in Fig. 2. Like in the linear case, a slow transfer (plots a,c) results in a robust NLT while a faster process (plots b,d) spoils the final state by dipole oscillations (b) or even breaks the inversion at all (d). However, the nonlinearity essentially changes rates of the process. The robust NLT are produced for larger barrier shifts ($1 \mu\text{m}$ instead of $0.013 \mu\text{m}$), for much shorter

times ($T=250$ ms instead of $T=1800$ ms for ideal BEC), and with much faster velocities ($\mu\text{m/s}$ instead of nm/s). The velocities are three order of magnitude higher (!) than in the linear case. The repulsive interaction greatly favors the population inversion (the transfer parameters become more comfortable for the experiment) and the effect is indeed huge. The reason is in the growth of the chemical potential μ , caused by the repulsive interaction. This leads to a dramatic increase of the barrier penetrability. The coupling between BEC fractions becomes strong and the inversion is realized much faster.

A more general information on NLT and is presented in Figs. 4 and 5 where the completeness P and noise n of the inversion are given for a wide range of velocity amplitudes. In Fig. 4, the sharp velocity profile $v_c(t)$ is used. Following the plots a,c) for the ideal BEC, a complete inversion ($P=1$) takes place only at a small velocity $v_0^c < 0.04 \mu\text{m/s}$. The inversion is somewhat spoiled by a noise $n = 0.02 - 0.04$ which weakens with decreasing the velocity. For $v_0^c > 0.04 \mu\text{m/s}$, we see a gradual destruction of the inversion, accompanied by an enhanced noise. For even larger velocities, the inversion breaks down ($P \rightarrow 0$) and the final state is characterized by strong Rabi oscillations ($n \rightarrow 0.4$). The oscillations are caused by the instant change of the velocity from zero to v_0^c at $t=0$ and back at $t=T$.

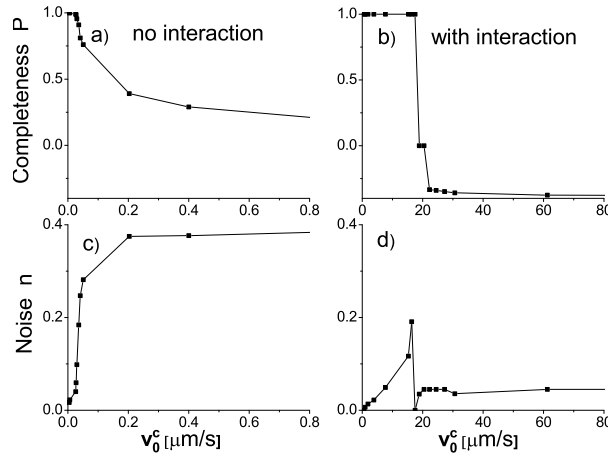


Figure 4. Completeness a)-b) and noise c)-d) of the population inversion for BEC without (left plots) and with (right plots) repulsive interaction versus the constant velocity $\bar{v}_a^c = v_0^c$.

Following Fig. 4 b,d), inclusion of the repulsive interaction dramatically changes the results. There appears a wide plateau, $0 < v_0^c \leq 19 \mu\text{m/s}$ (with the critical velocity $v^{\text{crit}} \approx 19 \mu\text{m/s}$), where the inversion is about complete ($P \approx 1$). As mentioned above, the repulsive interaction allows to get the inversion three orders of magnitude faster than for the ideal BEC. These findings are in accordance with our previous results for NLT, obtained within the simplified TMA model [14].

Note that in the ideal and repulsive BEC the inversion breaks down by different ways. While in the linear case the transfer completeness P tends not to zero, in the

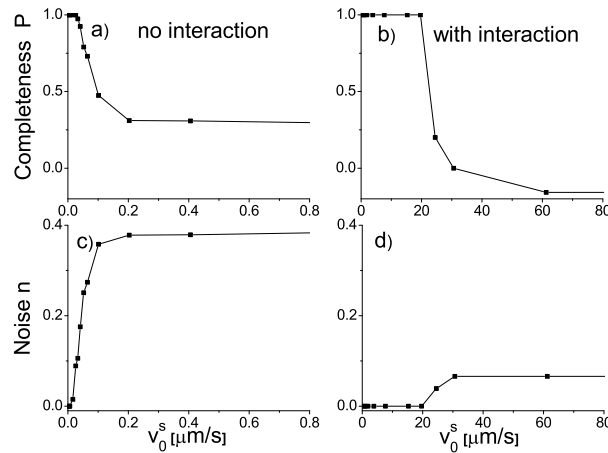


Figure 5. The same as in Fig. 4 but as a function of the *maximal* velocity v_0^s (profile $v_s(t)$).

repulsive BEC it becomes negative, $P \approx -0.7$. The later means that $z(0)$ and $z(T)$ have the same sign, i.e. the process results only in a partial population transfer, keeping the initial inequality $N_L > N_R$ at $t=T$.

In Figure 5, the similar analysis is done for the softer velocity profile $v_s(t)$. Note that, as compared to Figs. 2 and 3, here we use not the average v_a^s but maximal velocity $v_0^s = 2v_a^s$. The results are generally similar to those in Fig. 4. However, in the repulsive BEC (Fig. 5d), the process below the critical velocity is much less noised than in the previous $v_c(t)$ case. So, as might be expected, the softer (more adiabatic) profile $v_s(t)$ leads to a more robust inversion than the sharp profile $v_c(t)$.

In the repulsive BEC, the critical velocities for both profiles, $v_c^{\text{crit}} \approx 19 \mu\text{m/s}$ and $v_s^{\text{crit}} \approx 22 \mu\text{m/s}$, are rather similar. Note that these upper limits concern *maximal* (not average for $v_s(t)$) velocities. The physical sense of the critical velocity is simple: destruction of the adiabatic following [14]. Namely, if the system is transformed slowly, then the tunneling suffices to arrange BEC distribution in accordance to the transformation. Thus we gain the adiabatic NLT. However, at a critical velocity, the transformation becomes too fast and the efficient adiabatic transfer (transport) breaks down. This argument is partly confirmed by the fact that $v_c^{\text{crit}} < v_s^{\text{crit}}$, i.e. the softer velocity profile leads to a bigger critical velocity. More insight into the nature of v^{crit} can be reached by treating NLT in terms of Josephson direct and alternating currents [24], see the next subsection. Then v^{crit} is associated to the critical current manifesting the d.c. \rightarrow a.c. transition. However, d.c. also assumes an adiabatic following and so does not contradict the adiabatic arguments of Ref. [14].

3.3. Analogy to Josephson effects

Figure 6 shows evolution of the phase difference θ and Josephson currents for the successful NLT of ideal BEC, presented in Fig.2 a,c). Let's first consider the results for

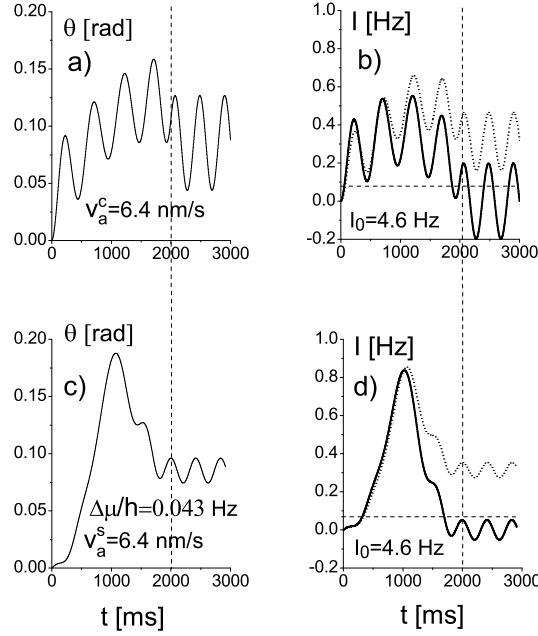


Figure 6. Evolution of the phase difference $\theta(t)$ (left) and Josephson currents (right) in the *ideal* BEC for the cases a) and c) of Fig. 2. The exact $I(t)$ (solid bold curve) and approximate $\tilde{I}(t)$ (dotted curve) currents are shown. In b,d), the critical current $I_0 = 4.6$ Hz is used to scale $\tilde{I}(t)$. For v_a^s (plot c), the chemical potential difference is indicated. The barrier shift duration $T=2$ s is marked by vertical dotted lines. For the reference, the zero line is given in b,d).

the soft velocity profile $v_s(t)$ (Fig.6 c,d). They are less damaged by dipole oscillations and so more convenient for the analysis. As seen from (c), the phase difference θ starts from zero at $t=0$, gets its maximum near the mid of the transfer ($t=T/2=1000$ ms) and then decreases to the value $\theta_T \sim 0.027$. This behavior roughly corresponds to the velocity profile, though the final θ does not return to zero but acquires a finite value θ_T . As shown below, the value of θ_T does not depend on barrier velocity. So most probably this is a geometric phase accumulated during the NLT. For $t > T$, the modest dipole oscillations take place.

Since θ varies with time, we have here a phase-running evolution, though with a small phase-locked ($\theta \approx \text{const}$) region at $t \sim T/2$. In the first half of the evolution ($t < T/2$), the average chemical potential difference is $\Delta\mu/h = \dot{\theta} \sim 0.043$ Hz, i.e. is very small. The d.c. assumes a constant phase difference θ and, therefore, zero chemical potential difference $\Delta\mu$. The present process demonstrates a small $\Delta\mu$ and so can be approximately treated as a quasiadiabatic d.c.. The true d.c. takes place only for shortly at the mid of the evolution ($t = T/2$).

Further insight to the process can be brought by a direct inspection of Josephson currents. In Fig. 6d), the exact current I obtained through \dot{z} and approximate current \tilde{I} determined through θ (see Eqs. (14) and (15)), are depicted. For calculation of \tilde{I} , the critical current $I_0 = 4.6$ Hz obtained from the condition $I(t) = \tilde{I}(t)$ at $t = T/2$ is used

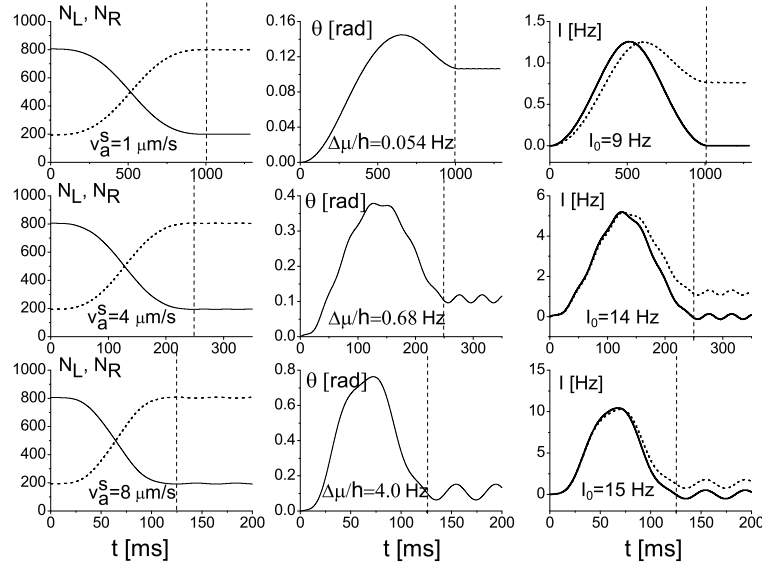


Figure 7. Evolution of the *repulsive* BEC for the soft velocity profile $v^s(t)$. Left plots: populations N_L (solid curve) and N_R (dash curve). Middle plots: phase difference θ . Right plots: exact I (bold solid line) and approximate \tilde{I} (dash line) Josephson currents. The slow ($v_a^s = 1 \mu\text{m/s}$, upper plots), middle ($v_a^s = 4 \mu\text{m/s}$, middle plots) and fast ($v_a^s = 8 \mu\text{m/s}$, bottom plots) processes are considered. For every case, the estimated chemical potential difference $\Delta\mu/h$ and critical current I_0 are given. The barrier shift durations are marked by vertical dash lines.

(note that maximal $I < I_0$). The plot d) shows that, for $t < T/2$, both I and \tilde{I} are similar and closely follow the evolution of θ . Since $I(t) \propto \sin \theta$, we indeed have here a Josephson-like phase-driven process.

For $t > T/2$, the behavior of I and \tilde{I} is different. I tends to zero (in accordance to Fig. 2c) while the approximate current \tilde{I} approaches a finite value (in accordance to behavior of θ in Fig. 3c). The difference is obviously caused by the final phase difference θ_T .

In Fig. a,b), the same characteristics are presented for the *constant* velocity. Despite the average velocities of two profiles are the same, $v_a^c = v_a^s = 6.4 \text{ nm s}^{-1}$, the evolution in (a,b) is very polluted by dipole oscillations, which once more shows the importance of using soft velocity profiles. In general, up to the dipole oscillations, the behavior of θ and currents in (a,b) is similar to those in (c,d). At the same time, the plot b) provides an additional information: it shows that the Josephson current I is not constant even for the constant velocity profile. So, in contrast to the statement [24], the Josephson current is not necessarily proportional to the barrier velocity.

In Figures 7 and 8, the evolution of the relevant characteristics for the *repulsive* BEC is presented. Since the velocity profile $v_c(t)$ leads to dipole oscillations which complicate the analysis, we will further inspect only the soft profile $v_s(t)$. In Fig. 7, the slow ($v_a^s = 1 \mu\text{m/s}$), middle ($v_a^s = 4 \mu\text{m/s}$) and fast ($v_a^s = 8 \mu\text{m/s} < v_{\text{crit}}$) evolutions are considered. In all the cases, a successful NLT takes place (left plots). The behavior of

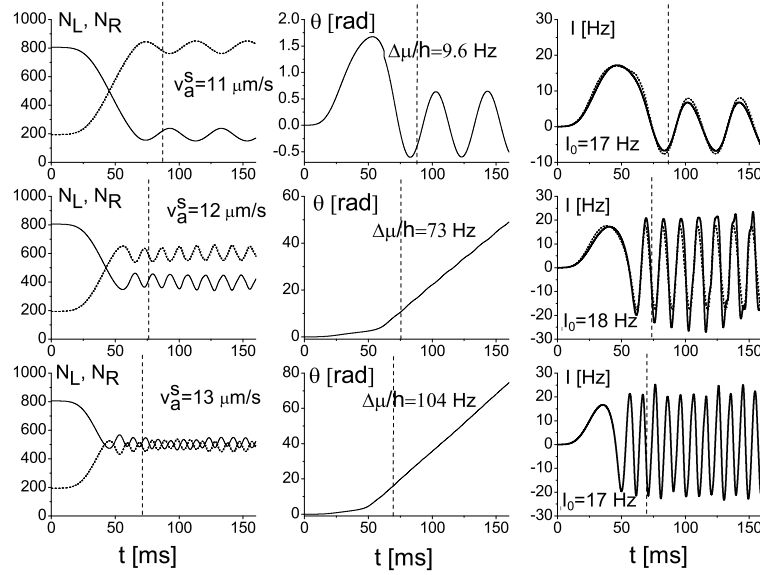


Figure 8. Evolution near the critical velocity. The same as in Fig. 7 but for average velocities $v_a^s = 11 \mu\text{m/s}$, (upper plots), $v_a^s = 12 \mu\text{m/s}$ (middle plots), and fast $v_a^s = 13 \mu\text{m/s}$ (bottom plots).

θ and currents in the repulsive BEC is qualitatively similar to those for the ideal BEC. The main difference is in a significant enhancement of the process rates. In particular, as mentioned above, the average barrier velocities become 3 orders of magnitude bigger than for the ideal BEC. The final phase difference θ_T remains constant with increasing v_a^s . Its relative impact, being decisive for a low velocity, becomes less important for large velocities. It seems that just θ_T leads to some variance of I_0 . For a large $v_a^s = 8 \mu\text{m/s}$, we still have $\theta < \pi/2$ and $I < I_0$. The chemical potential difference yet remains modest, $\Delta\mu/h \sim 4.0 \text{ Hz}$. So, in general agreement with the prediction [24], this NLT can be approximately treated as a quasiadiabatic phase-driven d.c.-like process.

In Figure 8, the NLT near v_a^{crit} is considered (for the soft velocity profile, this *average* critical velocity is twice smaller than the *maximal* critical velocity in Figs. 4-5). It is seen that at the interval $11 \mu\text{m/s} < v_a^s < 12 \mu\text{m/s}$ there is a pronounced transition to the a.c.-like regime. For $v_a^s \geq 12 \mu\text{m/s}$, θ acquires a linear time dependence while the current starts to oscillate with the frequency $\omega \approx \Delta\mu/h$. The value of $\Delta\mu$ becomes much larger than for $v_a^s < v_a^{\text{crit}}$. The approximate current \tilde{I} converges to the supercurrent I , while the later approaches the critical current I_0 . Altogether all these factors unambiguously indicate the a.c. nature of the final state. The high-frequency a.c. is modulated by low-frequency dipole oscillations. The a.c. looks like MQST [21, 23] (running phase, nonzero average population imbalance $\langle z \rangle$) near the critical point ($v_a^s = 12 \mu\text{m/s}$) but deviates from MQST ($\langle z \rangle \rightarrow 0$) at higher velocities.

Altogether, our analysis confirms that the NLT can be approximately treated as a phase-driven, quasiadiabatic, d.c.-like process occurring at $v < v^{\text{crit}}$. For higher velocities $v > v^{\text{crit}}$, the NLT breaks down and transforms to a.c. Note that the d.c.

treatment of NLT should be taken with a care. Indeed, our calculations show that, for $v < v^{\text{crit}}$, the phase difference θ is not constant and the chemical potential difference $\Delta\mu$ is not zero. Only smallness of $\dot{\theta}$ and thus $\Delta\mu$ permits the d.c. treatment.

It should be emphasized that a cornerstone of d.c. in a weakly coupled phase-driven system is an adiabatic following. Indeed, the d.c. is adiabatic by definition (as a weak current yet unable to produce quasiparticle excitations). Therefore, v^{crit} can be treated as a critical point for both d.c. \rightarrow a.c. [24] and (quasi)adiabatic \rightarrow nonadiabatic [14] transitions. Then, for example, the critical velocity in quasiadiabatic Landau-Zener population transfer of the repulsive BEC in a double-well trap [14] can be viewed both as a break of adiabatic following and as a d.c. \rightarrow a.c. transition.

Finally note that, in the present study, the trap is transformed from the initial asymmetric form to the final opposite asymmetric form, passing through the symmetric configuration at the mid of the process (asym \rightarrow sym \rightarrow -asym transformation). Instead, the previous theoretical [24] and experimental [27] studies used sym \rightarrow asym and asym \rightarrow sym transformations, respectively. Despite these differences, the Josephson physics behinds the evolutions is essentially the same. However, as compared to [24, 27], our analysis is more complete in the sense that i) the nonlinear impact is explored in detail and ii) the crucial ingredient of the Josephson effects, the phase difference, is numerically inspected.

4. Summary

The linear and nonlinear transport of BEC in a double-well trap was investigated within the time-dependent three-dimensional Gross-Pitaevskii equation, in close reference to parameters of Heidelberg experiments [31, 32]. The calculations are performed for the total order parameter, thus avoiding typical (two-mode, etc) approximations. The population transfer is driven by a time-dependent barrier shift with a sharp (rectangular) and soft ($\sim \cos^2(\omega t)$) velocity profiles. It is shown that using the soft profile is crucial to avoid strong dipole oscillations which significantly pollute the transport and complicate its theoretical analysis and experimental observation [27].

The calculations confirm our previous findings (obtained in the simplified model [14]) that repulsive interaction between BEC atoms (and related nonlinearity of the problem) significantly supports the NLT, making it possible in a wide interval of barrier velocities. As compared to the ideal BEC, the process can be three orders of magnitude faster. Besides, the nonlinearity allows to produce the transport between stationary states of essentially anisotropic trap. All these factors should facilitate experimental investigation of NLT.

Note that the interaction effect is mainly caused by the rise of the chemical potential. Hence the effect should depend on the barrier form, being strong for smooth barriers whose penetrability increases with the excitation energy and suppressed for sharp barriers with a slight energy dependence of the penetrability.

Further, the relation of NLT and d.c. Josephson effect was inspected in detail. As

compared to previous studies [22, 23, 24, 25, 26], the evolution of the phase difference θ (a crucial ingredient of the Josephson effect) was numerically explored. It was shown that, in accordance to [24, 27], the NLT indeed can be approximately treated as the d.c.. Above the critical barrier velocity v^{crit} , the NLT decays into the a.c.. Note that the d.c. treatment of NLT is actually an approximation because in NLT the phase difference θ is not constant and the chemical potential difference $\Delta\mu$ is not zero, which contradicts the d.c. definition. However, because of the smallness of $\dot{\theta}$ and $\Delta\mu$, the d.c. treatment is still reasonable.

The behavior of the transport near the critical velocity v^{crit} was investigated in detail. It is shown that v^{crit} marks both d.c. \rightarrow a.c. [24] and (quasi)adiabatic \rightarrow nonadiabatic [14] transitions. These results emphasize an adiabatic nature of d.c. in Bose-Josephson junctions (BJJ). Actually we deal here with a general phase-driven adiabatic following of weakly-bound two-component system. In this sense, a variety of (quasi)adiabatic population transfer protocols (from familiar Landau-Zener [11, 12] scheme and its generalizations [14] to modern adiabatic prescriptions [17]) in internal and external BJJ can be roughly considered as manifestations of the d.c. Josephson effect.

Acknowledgments

The work was partly supported by the RFBR grant 14-02-00723 and grants of University of Paul Sabatier (Toulouse, France). We thank Prof. D. Guéry-Odelin for useful discussions.

References

- [1] Petrick C J and Smith H 2002 *Bose-Einstein Condensation in Dilute Gases* (Cambridge: Cambridge University Press)
- [2] Pitaevskii L P and Stringari S 2003 *Bose-Einstein Condensation* (Oxford: Oxford University Press)
- [3] Dalfovo F, Giorgini S, Pitaevskii L P and Stringari S 1999 *Rev. Mod. Phys.* **71** 463
- [4] Leggett A J 2001 *Rev. Mod. Phys.* **73** 307
- [5] Courteille P W, Bagnato V S and Yukalov V I 2001 *Laser Phys.* **11** 659
- [6] Gati R and Oberthaler M K 2007 *J. Phys. B: At. Mol. Opt. Phys.* **40** R61
- [7] Torrontegui E, Ibáñez S, Martínez-Caraot S, Modugno M, del Campo A, Guéry-Odelin D, Ruschhaupt A, Xi Chen and Muga J G 2013 *Adv. At. Mol. Opt. Phys.* **62** 117
- [8] Dalibard J, Gerbier F, Juzeliūnas G and Öhberg P 2011 *Rev. Mod. Phys.* **83** 1523
- [9] Birman J L, Nazmitdinov R G and Yukalov V I 2013 *Phys. Rep.* **526** 1
- [10] Kral P, Thanopoulos I and Shapiro M 2007 *Rev. Mod. Phys.* **79** 53
- [11] Landau L D 1932 *Phys. Z. U.S.S.R.* **2** 46
- [12] Zener C 1932 *Proc. R. Soc. London, Ser. A* **137** 696
- [13] Nesterenko V O, Novikov A N, de Souza Cruz F F and Lapolli E L 2009 *Laser Phys.* **19** 616
- [14] Nesterenko V O, Novikov A N, Cherny A Y, de Souza Cruz F F and Suraud E 2009 *J. Phys. B: At. Mol. Opt. Phys.* **42** 235303
- [15] Ruschhaupt A, Xi Chen, Alonso D and Muga J G 2012 *New. J. Phys.* **14** 93040
- [16] Allen L and Eberly J H 1987 *Optical Resonance and Two-Level Atoms* (New York: Dover)
- [17] Berry M B 2009 *J. Phys. A: Math. Theor.* **42** 365303

- [18] Juliá-Díaz B, Martorell J and Polls A 2010 *Phys. Rev. A* **81** 063625
- [19] Yuste A, Juliá-Díaz B, Torrontegui E, Martorell J, Muga J G and Polls A 2013 *Phys. Rev. A* **88** 043647
- [20] Josephson B D 1962 *Phys. Lett.* **1** 251
- [21] Smerzi A, Fantoni S, Giovanazzi S and Shenoy S R 1997 *Phys. Rev. Lett.* **79** 4950
- [22] Zapata I, Sols F and Legett A J 1998 *Phys. Rev. A* **57** R28
- [23] Raghavan S, Smerzi A, Fantoni S and Shenoy S R 1999 *Phys. Rev. A* **59** 620
- [24] Giovanazzi S, Serzi A and Fantoni S 2000 *Phys. Rev. Lett.* **84** 4521
- [25] Meier F and Zwerger W 2001 *Phys. Rev. A* **64** 033610
- [26] Sakellari E, Leadbeater M, Kylstra N J and Adams C S 2002 *Phys. Rev. A* **66** 033612
- [27] Levy S, Lahoud E, Shomroni I and Steinhauer J 2007 *Nature* **449** 579
- [28] Pitaevskii L P 1961 *Sov. Phys.-JETP* **13** 451; Gross E P 1961 *Nuovo Cimento* **20** 454
- [29] Milburn G J, Corney J, Wright E M and Walls D F 1997 *Phys. Rev. A* **55** 4318
- [30] Yukalov V I, Marzlin K-P and Yukalova E P 2004 *Phys. Rev. A* **69** 023620
- [31] Albiez M, Gati R, Fölling J, Hunsmann S, Cristiani M and Oberthaler M K 2005 *Phys. Rev. Lett.* **95** 010402
- [32] Gati R, Albiez M, Fölling J, Hemmerling B and Oberthaller M K 2006 *Appl. Phys. B* **82** 207
- [33] Gross C 2012 *J. Phys. B: At. Mol. Opt. Phys.* **45** 103001
- [34] Werschnik J and Gross E K U 2007 *J. Phys. B: At. Mol. Opt. Phys.* **40** R175
- [35] Garcia-March M A, Mazzarella G, Dell'Anna L, Julia-Diaz B, Salasnich L and Polls A, arXiv:1401.7693v1 [cond-mat.quant-gas].
- [36] Radzihovsky L and Gurarie V 2010 *Phys. Rev. A* **81** 063609
- [37] Blum V, Lauritsch G, Maruhn J A and Reinhard P-G 1992 *J. Comput. Phys.* **100** 364
- [38] DeVries P L 1987 *AIP Conf. Proc.* **160** 269
- [39] Nesterenko V O, Novikov A N and Suraud E 2012 *J. Phys. B: At. Mol. Opt. Phys.* **45** 225303